

# High-resolution temperature-dependent Brillouin scattering studies of ferroelectric K<sub>3</sub>Nb<sub>3</sub>O<sub>6</sub>(B<sub>03</sub>)<sub>2</sub>

著者	Maczka M., Hanuza J., Kojima S.
journal or publication title	Physical review B
volume	77
number	10
page range	104116
year	2008-03
権利	(C)2008 The American Physical Society
URL	<a href="http://hdl.handle.net/2241/104066">http://hdl.handle.net/2241/104066</a>

doi: 10.1103/PhysRevB.77.104116

# High-resolution temperature-dependent Brillouin scattering studies of ferroelectric $K_3Nb_3O_6(BO_3)_2$

M. Maćzka

*Institute of Low Temperature and Structure Research, Polish Academy of Sciences, P.O. Box 1410, 50-950 Wrocław 2, Poland*

J. Hanuza

*Department of Bioorganic Chemistry, University of Economics, 53-345 Wrocław, Poland*

S. Kojima

*Institute of Materials Science, University of Tsukuba, Tsukuba, Ibaraki 305-8573, Japan*

(Received 3 December 2007; published 20 March 2008)

High-resolution micro-Brillouin scattering studies of  $K_3Nb_3O_6(BO_3)_2$ , exhibiting superionic and ferroelectric properties, were performed in the temperature range of 300–870 K. Strong increase in damping of longitudinal and transverse acoustic phonons corresponding to the  $c_{33}$  and  $c_{44}$  elastic constants was observed above 650 K. This increase in damping was correlated with anomalous decrease in the  $c_{33}$  and  $c_{44}$  elastic constants and strong increase in central peak intensities. The observed behavior has been attributed to melting of the  $K^+$  sublattice as a result of the order-disorder phase transitions. The obtained results also revealed a critical slowing down of the  $E''$ -symmetry relaxation mode near the phase transitions at 388 and 690 K as well as the broad  $A_1'$ -symmetry relaxation mode near the phase transition at 750 K. This behavior indicates that the relaxation modes play an important role in the mechanism of these phase transitions. In particular, this behavior suggests that the phase transition near 690 K is induced by instability of the  $E''$ -symmetry relaxation mode.

DOI: [10.1103/PhysRevB.77.104116](https://doi.org/10.1103/PhysRevB.77.104116)

PACS number(s): 78.35.+c, 65.40.Ba, 63.20.-e, 77.80.Bh

## I. INTRODUCTION

Boron containing compounds play an important role in modern nonlinear optics since these materials usually have high  $\chi^{(2)}$  and  $\chi^{(3)}$  nonlinear susceptibilities, outstanding resistance to laser damage, and a cut-off wavelength in the near-ultraviolet region.<sup>1–4</sup>  $K_3Nb_3O_6(BO_3)_2$  (KNBO) is a promising crystal for applications since it has recently been found to be an attractive  $\chi^{(3)}$ -active crystal for picosecond stimulated Raman scattering generation in the visible and near-IR region.<sup>5</sup> This material has also attracted considerable attention due to the presence of successive structural transitions at  $T_1=783$ ,  $T_2=750$ ,  $T_3=690$ ,  $T_4=388$ ,  $T_5=198$ , and  $T_6=80$  K.<sup>6–10</sup> The structure above 783 K was first reported as trigonal, space group  $P31m$ .<sup>11</sup> Later studies showed that this structure was incorrectly described as trigonal and it is most likely hexagonal,  $P62m=D_{3h}^{3,12,13}$ . The room temperature structure was determined as orthorhombic,  $P2_1ma=C_{2v}^{2,12}$ . Symmetries of the remaining phases are not certain, but it was previously suggested that the crystal symmetry changes into  $Pm$  and  $C2mm$  below 750 and 690 K, respectively.<sup>5</sup> Heat capacity, microscopic, dielectric, and conductivity studies showed that the phase transitions at  $T_3$  and  $T_5$  are first order transitions.<sup>8–10</sup> The character of the observed anomalies suggested also that the transition at  $T_2$  may be weakly first order, whereas the remaining transitions are close to second order.<sup>8–10</sup> These studies revealed also the presence of domains below 750 K and showed that KNBO displays below 783 K ferroelectric properties, with spontaneous polarization parallel to the hexagonal  $c$  axis. It was also noticed that the direction of the spontaneous polarization does not agree with the  $P2_1ma$  symmetry established for the room temperature phase. Temperature dependence of

conductivity indicated that KNBO might be a superionic conductor at higher temperatures.<sup>8,9</sup>

In the present paper, the temperature-dependent Brillouin scattering studies of KNBO are reported in order to understand the mechanisms of the phase transitions and to find out whether these transitions are related to relaxational phenomena. Such phenomena may also appear in the absence of any phase transitions and are often observed in superionic conductors.<sup>14–17</sup> Relaxation modes may give rise to a quasi-elastic light scattering, i.e., the so-called central peaks (CPs),<sup>14–19</sup> and analysis of the observed CPs may provide an evidence that a studied material exhibits superionic properties. It will be shown in the present paper that KNBO shows the presence of very clear CPs. The temperature dependence of these CPs and some acoustic modes proves that the studied crystal exhibits superionic properties. It also shows that the phase transitions at  $T_2$ ,  $T_3$ , and  $T_4$  have an order-disorder nature.

## II. EXPERIMENT

KNBO crystals were grown from the flux. The mixture of  $K_2CO_3$ ,  $Nb_2O_5$ , and  $B_2O_3$ , corresponding to the composition  $K_3Nb_3O_6(BO_3)_2$  and  $K_2B_4O_7$  in a ratio of 1:1, was placed in a platinum crucible, heated to 1000 °C, kept in this temperature for 40 h, cooled with a rate of 2–840 °C, and then cooled with a rate 10 °C to room temperature. The obtained crystals were extracted from the crucible by washing with hot water. Single crystals had form of hexagonal rods up to 5 mm in length and up to  $2 \times 2$  mm<sup>2</sup> in cross section.

The Brillouin spectra were obtained with a 3+3 pass tandem Sandercock-type Fabry–Perot interferometer combined with an optical microscope. The free spectral ranges (FSRs)

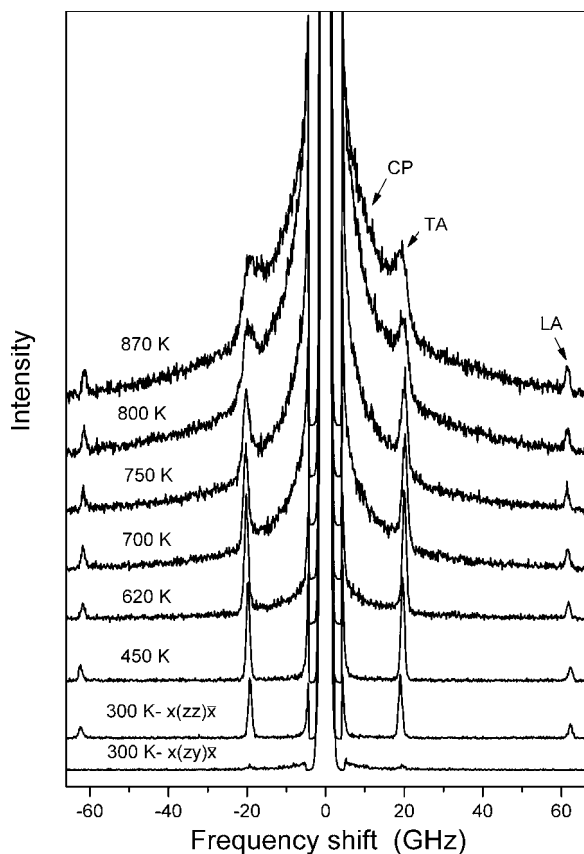


FIG. 1. Example of the temperature dependence of the  $x(zz+z\bar{y})\bar{x}$  Brillouin spectra for KNBO. The polarized  $x(zz)\bar{x}$  and  $x(z\bar{y})\bar{x}$  spectra measured at 300 K are also presented to show the polarization behavior of the acoustic modes.

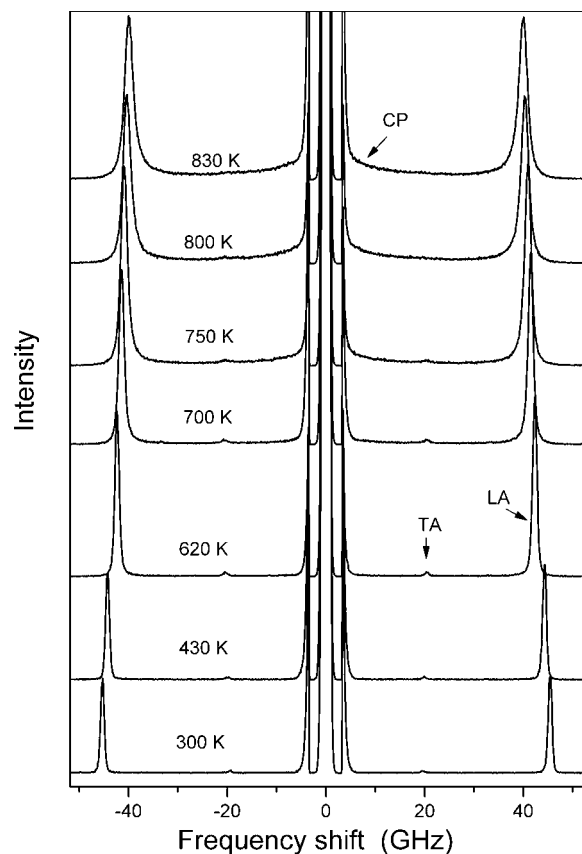


FIG. 2. Example of the temperature dependence of the  $z(yy+yx)\bar{z}$  Brillouin spectra for KNBO.

### III. RESULTS

of 40, 60, 100, 150, and 500 GHz were employed. The scattered light from the sample was collected in the back-scattering geometry. A conventional photon-counting system and a multichannel analyzer were used to detect and average the signal. The samples were set in a cryostat cell (THMS 600). The sample cell with X-Y adjustment was placed onto the stage of an optical microscope (Olympus BH-2) having Z adjustment. The Brillouin spectra were obtained for 1024 channels after 500 time repetitions of accumulation with a gate time of 500 ms for one channel. More details of experimental setup can be found in our previous paper.<sup>20</sup>

The frequency shifts, full width at half maximum (FWHM), and intensity of the Brillouin peaks corresponding to longitudinal acoustic (LA) and transverse acoustic (TA) modes were evaluated by fitting the measured spectra to the convolution of the Gaussian instrumental function with a theoretical spectral line shape that is Lorentzian in form.<sup>21</sup> Half-widths and intensity of the CPs were evaluated by fitting the spectra to the Lorentzian function. Sound velocities and corresponding elastic constants were calculated from the measured frequency shifts using the mass density of  $3.845 \times 10^3 \text{ kg/m}^3$  and the refractive indices  $n_o=1.875$  and  $n_e=1.862$ .<sup>5,12</sup>

Typical Brillouin spectra of the KNBO crystal in  $x(zz+z\bar{y})\bar{x}$  and  $z(yy+yx)\bar{z}$  scattering geometries are shown in Figs. 1 and 2, where  $x$  and  $z$  correspond to the  $a$  and  $c$  hexagonal axes, respectively, whereas  $y$  is perpendicular to  $a$  and  $c$ . In the  $z(yy+yx)\bar{z}$  scattering geometry, a strong peak is observed near 45.4 GHz which can be assigned to the LA mode corresponding to the  $c_{33}$  elastic constant. Another, very weak TA peak, corresponding to the  $c_{44}$  elastic constant, is observed near 19.5 GHz. In the  $x(zz+z\bar{y})\bar{x}$  scattering geometry, two peaks are observed: a strong peak near 19.6 GHz, i.e., at the frequency very similar to the frequency of the  $c_{44}$  mode propagating along the  $z$  direction, and a weak peak near 62.31 GHz. These peaks are strongly polarized; i.e., they appear for the  $x(zz)\bar{x}$  polarization and disappear for the  $x(z\bar{y})\bar{x}$  polarization (see Fig. 1). According to the selection rules for the  $P6_2m$  structure,<sup>22,23</sup> only the LA mode corresponding to the  $c_{11}$  elastic constant should be observed in the  $x(zz)\bar{x}$  polarization. We assign to this mode the higher frequency Brillouin peak at 62.31 GHz. The lower frequency peak should be assigned to a TA mode. In this scattering geometry, two transverse modes correspond to the  $c_{44}$  and  $c_{66}$  elastic constants of the hexagonal phase.<sup>21,22</sup> They are forbidden to be observed for the  $D_{3h}^3$  and orthorhombic phases, but they could appear as a result of the monoclinic or triclinic distortion of the crystal structure from the hexagonal

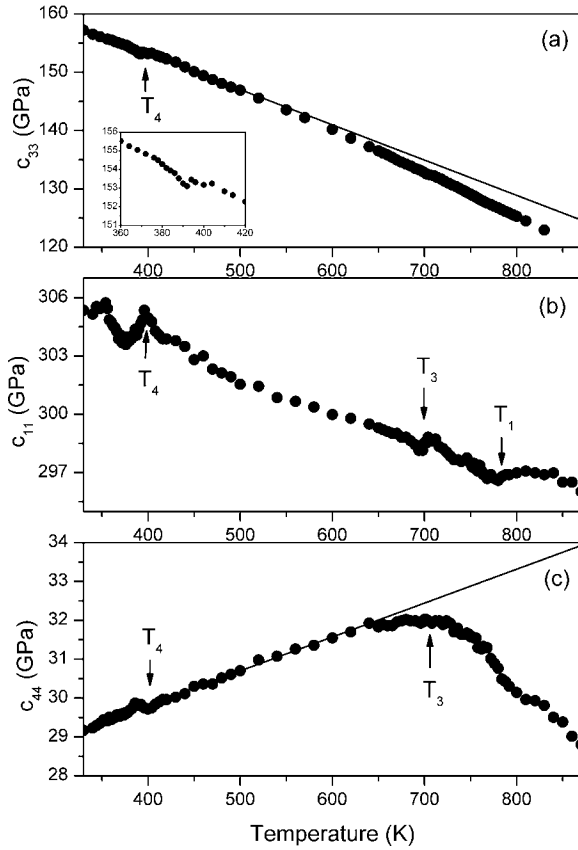


FIG. 3. Temperature dependence of the (a)  $c_{33}$  (b)  $c_{11}$ , and (c)  $c_{44}$  elastic constants. The solid lines represent linear fitting of the experimental data below 600 K. The inset shows the anomaly of the  $c_{33}$  constant near  $T_4$ .

symmetry.<sup>22</sup> In case of the monoclinic structure, the  $c_{66}$  mode could appear for the  $x(z\bar{y})\bar{x}$  polarization, whereas the  $c_{44}$  should be present for the  $x(z\bar{z})\bar{x}$  polarization.<sup>22,24</sup> Frequency of this mode and its polarization behavior indicate that it corresponds to the  $c_{44}$  elastic constant. Using the obtained data and assuming the pseudohexagonal symmetry, we were able to estimate the  $c_{11}$ ,  $c_{33}$ , and  $c_{44}$  elastic constants at 300 K as 304.7, 159.3, and 29.5 GPa, respectively. These values are much higher than those typically observed for borates (for example, the highest values of the elastic constants for  $\text{Li}_2\text{B}_4\text{O}_7$  and  $\beta\text{-BaB}_2\text{O}_4$  are 132.9 and 123.8 GPa, respectively<sup>25,26</sup>). They are, however, of similar magnitude as elastic constants of orthorhombic  $\text{KNbO}_3$  for which the highest value was 273 GPa for  $c_{22}$ .<sup>27</sup>

The plots presented in Fig. 3 show a decrease in the  $c_{33}$  and  $c_{11}$  elastic constants upon heating with some additional weak anomalies around  $T_1$ ,  $T_3$ , and  $T_4$  for the  $c_{11}$  elastic constant and around  $T_4$  for the  $c_{33}$  elastic constant. The  $c_{44}$  constant exhibits increase of up to 690 K and then decrease above this temperature. Very weak anomaly is also observed around  $T_4$ . Intensity of the TA mode corresponding to the  $c_{44}$  elastic constant (divided by  $n(\omega)+1$ , where  $n(\omega)=1/[\exp(h\omega/k_B T)-1]$  is the Bose factor) remains nearly constant in the whole temperature range studied. On the other hand, the plot of intensity of the LA mode corresponding to the  $c_{33}$  elastic constant as a function of temperature

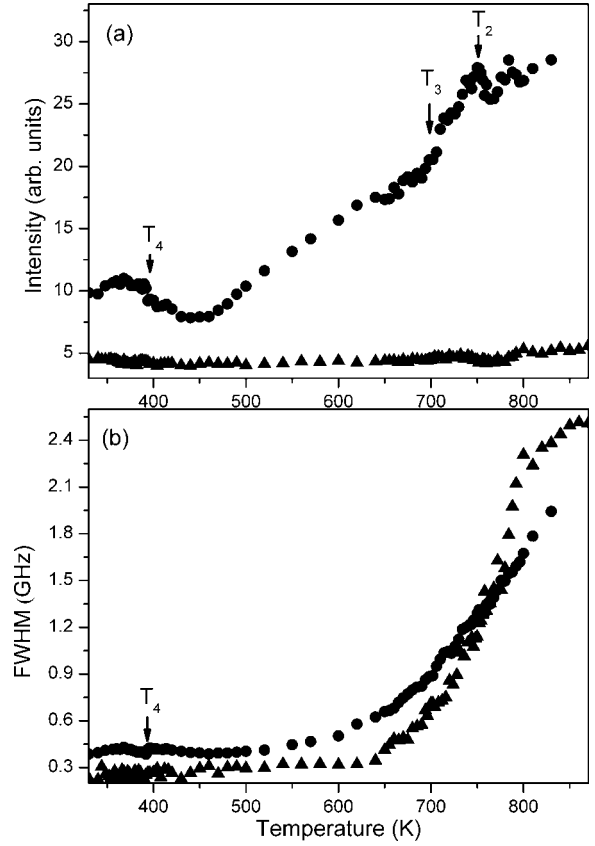


FIG. 4. Temperature dependence of (a) intensity [divided by the Bose-Einstein factor  $n(\omega)+1$ ] and (b) FWHM for the acoustic phonons corresponding to the  $c_{33}$  (circles) and  $c_{44}$  (triangles) elastic constants.

shows a peak below  $T_4$  and large increase above 450 K with some additional anomalies around  $T_3$  and  $T_2$  (see Fig. 4). Very interesting behavior is observed for temperature dependence of FWHM of the acoustic modes. Intensity of the  $c_{11}$  mode is weak and, therefore, we could not reliably establish the temperature dependence of FWHM for this mode. Nevertheless, our studies show that the FWHM changes little for this mode. In contrast to the  $c_{11}$  mode, the  $c_{44}$  and  $c_{33}$  modes exhibit very strong increase in FWHM at higher temperatures without any clear singularities around  $T_1$ ,  $T_2$ , and  $T_3$ . The FWHM for the  $c_{33}$  mode shows, however, an additional and weak anomaly near 394 K, which corresponds to the  $T_4$  phase transition.

As can be noticed in Figs. 1 and 2, at higher temperatures, a very clear CP is observed in the  $x(z\bar{z}+z\bar{y})\bar{x}$  scattering geometry, whereas in the  $z(yy+y\bar{x})\bar{z}$  geometry, the CP is very weak. In order to study these features, we have repeated the measurements using much larger FSR (see Figs. 5 and 6). Figure 6 shows that the  $x(z\bar{y})\bar{x}$  spectrum at 870 K can be approximated very well with only one Lorentzian with FWHM near 23 GHz. This CP corresponds to the  $E''$ -symmetry relaxation mode in the hexagonal phase. Only one CP is also observed in the  $x(yy)\bar{x}$  polarization. This CP corresponds to the  $A'_1$ -symmetry mode and its FWHM is also near 23 GHz at 870 K. In the  $x(z\bar{z})\bar{x}$  polarization, two  $A'_1$ -symmetry CPs are observed. FWHM of the narrow com-

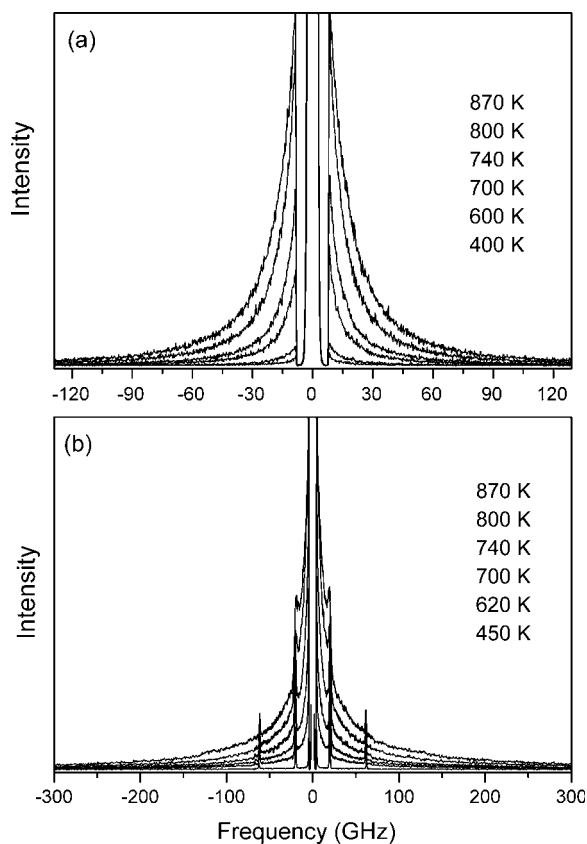


FIG. 5. Typical (a)  $x(zy)\bar{x}$  (FSR of 150 GHz) and (b)  $x(zz)\bar{x}$  (FSR of 500 GHz) Brillouin spectra at different temperatures.

ponent is the same as that observed in the  $x(yy)\bar{x}$  polarization. The second CP is much broader, i.e., its FWHM is about 220 GHz at 870 K. The polarization studies show that the ratio of integrated intensities of the narrow CP measured in  $x(zy)\bar{x}$ ,  $x(zz)\bar{x}$ , and  $x(yy)\bar{x}$  geometries is 85:48:100. The broad CP is weaker and the ratio of its integrated intensity to the intensity of the narrow CP measured in  $x(zz)\bar{x}$  polarization is approximately 70:100.

The CPs have Lorentzian-type shapes centered at the zero frequency shift that is indicative of a Debye relaxation. In this case, the relaxation time  $\tau$  can be estimated from a FWHM which is equal to  $1/\pi\tau$ .<sup>18,19</sup> Figure 7 presents temperature dependence of integrated intensity, FWHM, and  $1/\tau$  obtained from the fitting of the CPs to the Lorentzians [the reliable fitting of the  $A'_1$ -symmetry CPs could not be obtained below 620 K due to weak intensity of these peaks and simultaneous presence of the Brillouin lines in the  $x(zz)\bar{x}$  polarization].

#### IV. DISCUSSION

##### A. Central peaks

There are various mechanisms for the CPs in solids such as heat conduction mode, second order difference Raman scattering, collective motions of atoms associated with order-disorder phase transitions, and ion hopping.<sup>14,16,28-31</sup> If CP is due to heat conduction process, the FWHM should be pro-

portional to the square of the wave vector transfer.<sup>28,30</sup> The small size of the studied crystals did not allow us to check the dependence of the FWHM on the wave vector. Since, however, former studies showed that FWHM of CP due to heat diffusion is usually much smaller than in our case,<sup>30,32</sup> and its bandwidth should decrease with increasing temperature,<sup>30</sup> the assignment of the CP to this origin is unlikely. If CP is due to the second order Raman effect, its bandwidth usually extends to a few  $\text{cm}^{-1}$  at room temperature.<sup>16,30</sup> Our former vibrational studies of KNBO showed that bandwidths of the Raman lines very quickly increase with increasing temperature for this material up to even  $30 \text{ cm}^{-1}$  at 550 K temperature.<sup>33</sup> Therefore, it can be expected that the second order Raman processes would lead to appearance of a very broad CP at high temperatures. Since at high temperatures the FWHMs of the narrow and broad CPs are still below  $0.8$  and  $7.5 \text{ cm}^{-1}$  (24 and 220 GHz), respectively, the CPs cannot be assigned to the second order Raman scattering. The observed bandwidth of the CPs could indicate that these peaks originate from the polarization fluctuations associated with the order-disorder ferroelectric phase transitions. In this case, clear anomalies in intensity and decrease in the FWHM should be observed when the phase transition temperature is approached from below.<sup>19,34,35</sup> Weak anomaly in intensity near  $T_3$  for the  $E''$ -symmetry CP, the observed temperature dependence of the FWHM of the  $E''$ -symmetry CP near  $T_4$  and  $T_3$ , as well as the temperature dependence of the FWHM of the broad  $A'_1$ -symmetry CP near  $T_2$  (see Fig. 7) could be explained as arising from the polarization fluctuations (see discussion below). However, the strong increase in the CP intensity above  $T_3$  and its increase even above the highest transition temperature  $T_1$  must have a different origin. Since conductivity studies revealed a jump increase in the ionic conductivity for KNBO above  $T_3$ ,<sup>9</sup> typical for superionic conductors, we may conclude that at higher temperatures, the main contribution to the CPs comes from increased hopping of the  $\text{K}^+$  ions.

Huberman and Martin showed that CPs in superionic materials may have two different origins.<sup>14</sup> One type of CP arises from the charged density fluctuations. The second type of CP is related to fluctuations in the local site populations of conducting ions, the so-called pseudospin-density fluctuations.<sup>14</sup> These pseudospin fluctuations can be divided into two cases: ions may fluctuate between energetically inequivalent sites or equivalent sites. Redistribution of ions among inequivalent or equivalent sites leads to appearance of a polarized or depolarized CP, respectively.<sup>14</sup> The distinguishing between the two types of CPs is possible by choosing different scattering geometries. Moreover, the both types of CPs have much different widths, i.e., the CPs due to the charged density fluctuations are usually very narrow, even at high temperatures, whereas the CPs due to the pseudospin fluctuations extend up to acoustic mode frequencies.<sup>14,16,17,36</sup> The structure of KNBO contains large tunnels occupied by  $\text{K}^+$  ions which run parallel to the pseudo-hexagonal  $c$  axis. As a result, KNBO exhibits high ionic conductivity in the  $z$  direction.<sup>8</sup> If the narrow  $A'_1$ -symmetry CP was due to the charged density fluctuations, it should be strong in  $z(yy+yx)\bar{z}$  polarization because of high diffusion in the  $z$  direction. However, it is strong in  $x(yy)\bar{x}$  and  $x(zz)\bar{x}$  scattering



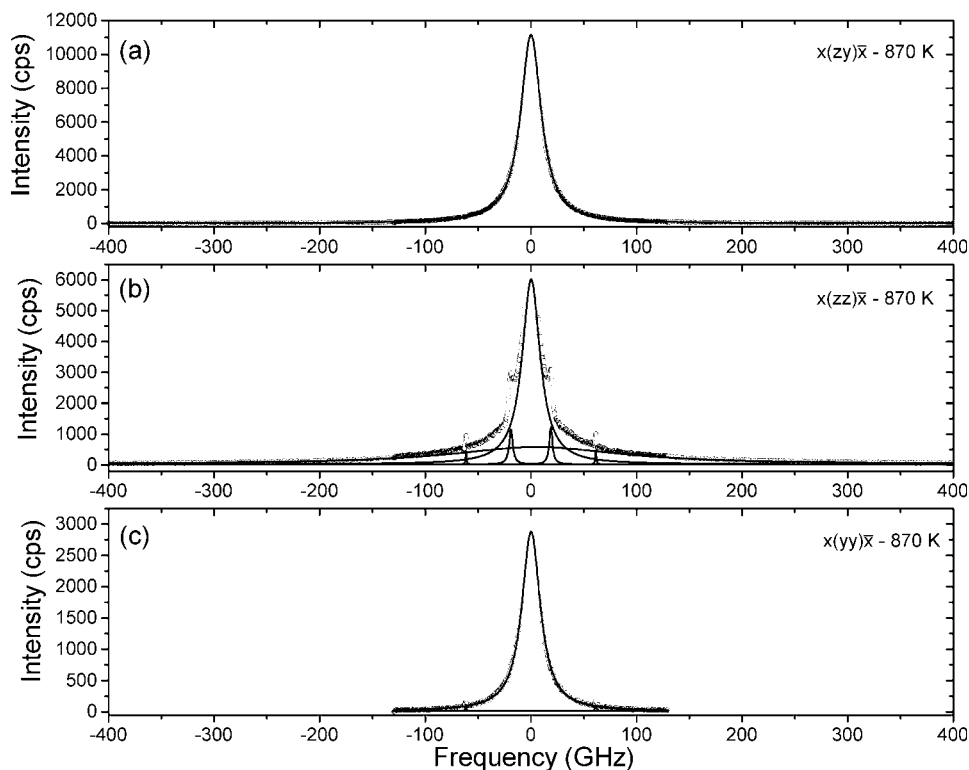


FIG. 6. (a)  $x(z\bar{y})\bar{x}$  (FSR of 500 GHz), (b)  $x(z\bar{z})\bar{x}$  (FSR of 500 GHz), and (c)  $x(y\bar{y})\bar{x}$  (FSR of 150 GHz) experimental spectra (circles) measured at 870 K. The solid lines show results of fitting of the CPs and acoustic modes to the Lorentzian shapes.

geometries but very weak in  $z(y\bar{y}+y\bar{x})\bar{z}$  polarization. The polarization behavior and large width of this CP (23 GHz at 870 K) indicate that it cannot be attributed to the charged density fluctuations but rather to pseudospin-density fluctuations. The large increase intensities of the broad  $A_1'$ -symmetry CP as well as the  $E''$ -symmetry CP above  $T_1$  indicates that also these peaks originate at high temperatures mainly from pseudospin-density fluctuations. The observation of both polarized and depolarized CPs indicates that the hopping of ions in KNBO occurs both between equivalent and inequivalent sites.

As can be noticed in Fig. 7, FWHM of the  $E''$ -symmetry CP significantly increases above  $T_3$ . However, it exhibits also an additional decrease in FWHM when  $T_3$  temperature is approached from below and a very clear anomaly is observed near  $T_4$ . Very similar temperature dependence of FWHM is also observed for the broad  $A_1'$ -symmetry CP near  $T_2$ . Such anomalies cannot be explained by assuming that the CPs entirely originate from the pseudospin fluctuations. However, linear dependence of  $1/\tau$  as a function of temperature is predicted by the Landau theory near the ferroelectric phase transitions.<sup>37</sup> Such behavior is known as a “critical slowing down” where  $1/\tau$  can be described by formula<sup>38,39</sup>

$$\tau = \frac{\tau_0 T_0}{|T - T_0|}. \quad (1)$$

Figure 7 shows, therefore, that at low temperatures, the main contribution to the observed temperature dependence of FWHM of the  $E''$ -symmetry CP is due to the fluctuations of the polarization and a very clear critical slowing down is observed near  $T_4$ . When temperature increases, contribution from the pseudospin-density fluctuations increases and there-

fore the critical slowing down is less clearly observed at  $T_3$ . The same arguments can be used to explain the temperature dependence of FWHM and intensity of the broad  $A_1'$ -symmetry CP near  $T_2$ . The observation of critical slowing down is direct evidence that the phase transitions at  $T_2$ ,  $T_3$ , and  $T_4$  have a significant contribution of an order-disorder mechanism. This picture is in agreement with the work of Huberman and Martin.<sup>14</sup> These authors showed that when a superionic conductor displays a phase transition, the correlation functions should diverge, giving rise to the usual narrowing of the CP near  $T_c$  and mixing of different relaxation processes for the fluctuations. Since the contribution of the pseudospin fluctuations to the CPs is negligible at low temperatures, it is reasonable to fit the data near  $T_4$  for the  $E''$ -symmetry mode with Eq. (1). Best fit to the experimental data below and above  $T_4$  gives  $T_0=449$  K ( $\tau_0=5.7$  ps) and  $T_0=324$  K ( $\tau_0=11.9$  ps), respectively. The relaxation time in KNBO is about 2 orders of magnitude longer than that typically observed for order-disorder phase transitions. For instance,  $\tau_0$  are 0.12 ps for  $\text{KH}_2\text{PO}_4$  (Ref. 40) and 0.096 ps for triglycine sulfate.<sup>41</sup> Significantly longer relaxation times are, however, observed when a relaxation mode couples to another mode. For example, for the tetragonal phases of  $\text{KD}_2\text{PO}_4$  and  $\text{K}_2\text{MgWO}_2(\text{PO}_4)_2$ ,  $\tau_0$  are 1.3 and 3.8 ps, respectively.<sup>42,43</sup> In case of KNBO, the long relaxation time can be most likely attributed to coupling between the relaxation modes related to the polarization and pseudospin-density fluctuations. It is also worth noting that the ratio of  $\tau_0$  in the phase stable above  $T_4$  to  $\tau_0$  in the phase stable below  $T_4$  is close to 2 (2.09), which shows that the phase transition at  $T_4$  should be close to a second order one.

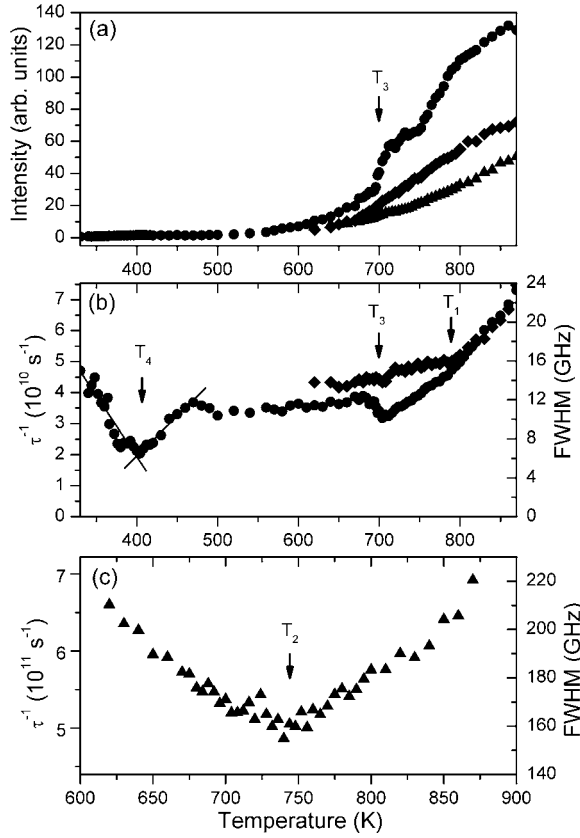


FIG. 7. (a) Temperature dependence of intensity of the  $E''$ -symmetry CP [ $x(z\bar{y})\bar{x}$  polarization, circles], the narrow  $A_1'$ -symmetry CP [ $x(zz)\bar{x}$  polarization, diamonds], and the broad  $A_1'$ -symmetry CP [ $x(zz)\bar{x}$  polarization, triangles]. (b) Temperature dependence of the inverse of the relaxation time estimated from FWHM of the  $E''$ -symmetry (circles) and the narrow  $A_1'$ -symmetry (diamonds) modes. Solid lines are fits to Eq. (8). (c) Temperature dependence of the inverse of the relaxation time estimated from FWHM of the broad  $A_1'$ -symmetry CP.

### B. Acoustic anomalies

The observation of the weak anomalies in temperature dependence of the elastic constants and intensities of the Brillouin lines as well as the weak anomaly in FWHM near  $T_4$  for the  $c_{33}$  mode (see Figs. 3 and 4) can be attributed to onset of the phase transitions. Weakness and shape of these anomalies indicate that the coupling between the acoustic modes and the order parameter is linearly quadratic.

Apart from the weak anomalies in elastic constants, the  $c_{44}$  constant exhibits also a very broad anomaly, i.e., this constant increases up to 690 K and then decreases above this temperature (see Fig. 3). Moreover, strong increase in damping of the acoustic phonons corresponding to the  $c_{33}$  and  $c_{44}$  constants is observed above 600 and 650 K, respectively (see Fig. 4). Since this behavior is correlated with strong intensity increase in the CPs, it can be attributed to coupling between the CPs and acoustic modes. According to Huberman and Martin, the shape of the spectrum resulting from the coupling between an acoustic mode and a CP related to pseudospin-density fluctuations is a superposition of a

Lorentzian centered at zero frequency and two other Lorentzians centered at frequencies  $+\omega_p$  and  $-\omega_p$  [see Eq. (9) of Ref. 14]. The first Lorentzian corresponds to the CP with FWHM equal to  $2\gamma$  where  $\gamma$  denotes the relaxation frequency for fluctuations, and the other Lorentzians correspond to the Brillouin peaks. The coupled acoustic phonon frequency is

$$\omega_p = \omega_k - \frac{n_0 A^2}{\rho v_s^2 k_B T} \frac{\omega_k \gamma^2}{\omega_k^2 + \gamma^2} \left( 1 + i \frac{\omega_k}{\gamma} \right), \quad (2)$$

where  $n_0$ ,  $\rho$ ,  $v_s$ ,  $k_B$ ,  $\omega_k$ , and  $A$  denote average density of mobile ions, density of the material, the phonon velocity, the Boltzmann constant, the uncoupled acoustic phonon frequency, and the coupling constant. The imaginary part of Eq. (2) gives information about damping of acoustic phonons and the real part about frequency shift due to the coupling. In principle, fitting of the recorded spectra to the coupled CP-acoustic mode response function [Eq. (9) of Ref. 14] should be performed to obtain information about temperature dependence of  $\omega_k$ ,  $\gamma$ ,  $n_0$ , and three coupling constants. The large number of fitting parameters makes such analysis not very reliable and, therefore, we present in our paper a simplified but more precise analysis with Lorentzian functions. This analysis provides information on temperature dependence of  $\omega_p$  (and related  $c_{ij}$  elastic constants),  $\gamma$ , CP intensity, and acoustic mode dampings. According to Eq. (2),  $\omega_p$  (damping) should exhibit decrease (increase) in comparison with the uncoupled values. The anomalous increase in damping is very clearly observed at high temperatures for the acoustic phonons of KNBO corresponding to the  $c_{33}$  and  $c_{44}$  elastic constants (see Fig. 4). It is, however, weak below 600 K indicating weak coupling of the acoustic phonons to the CPs below this temperature. We may assume, therefore, that the  $c_{33}$  and  $c_{44}$  values below 600 K approximately correspond to the bare elastic constants which are expected to exhibit a linear temperature dependence.<sup>44</sup> The best fit of the experimental data to  $c(T) = c(0) + mT$  yields  $c(0) = 26.3$  GPa ( $m = 0.0087$ ) for the  $c_{44}$  elastic constant and  $c(0) = 177.3$  GPa ( $m = -0.061$ ) for the  $c_{33}$  elastic constant. As can be noticed in Fig. 3, a clear departure from the linear behavior is observed above 600 and 650 K for the  $c_{33}$  and  $c_{44}$  elastic constants, respectively, i.e., above the same temperatures as the anomalous damping. Figure 8 shows more clearly that the temperature dependence of the anomalous parts of the elastic constants,  $\Delta c_{33}$  and  $\Delta c_{44}$ , is very similar to the temperature dependence of the acoustic phonon damping, presented in Fig. 4. It is also worth noting that the plot of the  $\Delta c_{44}$  as a function of temperature exhibits a clear change in the slope near 780 K, which reflects the onset of the phase transition at  $T_1$ . An anomaly near  $T_1$  is also observed for the  $\Delta c_{33}$ . Changes in the slopes near  $T_1$  are also observed for the  $E''$ -symmetry CP as well as the narrow  $A_1'$ -symmetry CP (see Fig. 7). All these facts confirm our conclusions that the observed strong increase in damping of the acoustic phonons and their anomalous frequency decrease have the same origin, i.e., they are due to coupling of the acoustic modes to the relaxation modes observed as CPs in the present studies. It is worth noting that the former studies revealed a very

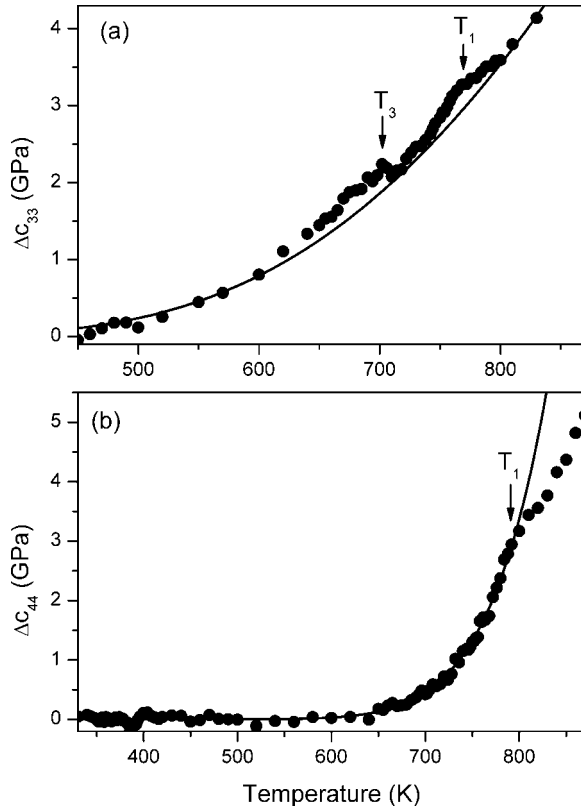


FIG. 8. Temperature dependence of the anomalous parts of  $c_{33}$  (a) and  $c_{44}$  (b) elastic constants obtained after subtraction of the experimental data from the values estimated from the linear fits presented in Fig. 3. Solid lines are fits to Eq. (4).

similar temperature dependence of acoustic mode dampings and frequency shifts, as those observed for KNBO, at the transition into a superionic phase of  $\alpha$ -AgI.<sup>45</sup> This result supports our conclusion that the observed strong acoustic anomalies in KNBO can be attributed to increased hopping of the ions due to the onset of the order-disorder transition at  $T_3$  associated with melting of the  $K^+$  sublattice.

It has previously been shown that the anomalous decrease in acoustic mode frequency  $\Delta\omega(T) = \omega_k - \omega_p$  due to coupling between an acoustic mode and a relaxation mode can be well approximated in a superionic conductor by the Arrhenius law,<sup>46</sup>

$$\Delta\omega(T) = C \exp\left(\frac{-E_a}{k_B T}\right), \quad (3)$$

where  $C$  is the proportionality coefficient and  $E_a$  is the activation energy. Since elastic constant is proportional to the square of the phonon frequency,  $\Delta c_{ij}(T)$  could be approximated by the formula

$$\Delta c_{ij}(T) = D \exp\left(\frac{-2E_a}{k_B T}\right), \quad (4)$$

where  $D$  is the proportionality coefficient. Figure 8 shows that the temperature dependence of  $\Delta c_{44}$  below 780 K can be well described by Eq. (4) with the activation energy  $E_a$

$= 0.48$  eV. The fitting of the  $\Delta c_{33}$  gives  $E_a = 0.16$  eV. The value of the activation energy obtained from the fitting of  $\Delta c_{44}$  is in good agreement with the value estimated from conductivity normally measured to the  $c$  axis (0.43 eV).<sup>8</sup> This result indicates that behavior of  $\Delta c_{44}$  can indeed be well explained by ionic-acoustic interactions, and the coupling between the order parameter and acoustic phonon corresponding to the  $c_{44}$  elastic constant is weak. The value of the activation energy estimated from the temperature dependence of  $\Delta c_{33}$  seems to be too small. Possibly, this is caused by stronger coupling of the LA phonon corresponding to the  $c_{33}$  elastic constant to the order parameter as well as inaccuracy in estimation of  $\Delta c_{33}$ .

### C. Mechanism of the phase transitions and possible symmetry changes

The observed acoustic anomalies and temperature dependence of the CPs do not give answers regarding possible symmetry changes at  $T_1$  and  $T_2$ . The observation of very clear slowing down for the broad  $A'_1$ -symmetry CP near  $T_2$  indicates, however, that this mode plays an important role in the mechanism of the phase transition at  $T_2$ . Since this mode is observed only in the  $x(zz)\bar{x}$  polarization, it involves ionic motion in the  $c$  direction, i.e., along the polar axis. This kind of collective motion of ions is the origin of the very strong dielectric anomaly, observed previously.<sup>8,9</sup> As far as the phase transitions at  $T_3$  and  $T_4$  are concerned, the observation of critical slowing down for the relaxation mode observed in  $x(yz)\bar{x}$  polarization indicates that this mode plays a major role in the mechanism of these phase transitions. This mode is related to the  $E''$ -symmetry excitation in the hexagonal phase involving motions within the  $xy$  plane. If a group-subgroup relation is fulfilled for this transition, as suggested in previous papers,<sup>5,9,10</sup> instability of the  $E''$ -symmetry mode could lead to point symmetry lowering into a triclinic ( $C_1$ ) or monoclinic ( $C_2$  or  $C_s$ ) structures. In the triclinic structure, the spontaneous polarization  $P_s$  may have a general direction. In the  $C_2$  structure,  $P_s$  should be along the  $y$  direction and in the  $C_s$  structure within the  $yz$  plane. Since the dielectric permittivity showed the pronounced anomaly only along the  $z$  direction,<sup>8,9</sup> we may exclude the  $C_2$  possibility. Therefore, the phase transition at  $T_3$  could occur into  $C_s$  or  $C_1$  structures. Although, for these structures, some component of  $P_s$  in the direction perpendicular to the  $z$  direction is expected, it might be much weaker than that along the  $z$  direction. The  $C_s$  or  $C_1$  point symmetries were indeed suggested below  $T_3$  on the basis of domain structure observations by Kharitonova *et al.*<sup>9</sup> If we assume  $Pm$  symmetry, the  $E''$ -symmetry CP should split below  $T_3$  into  $A'$  and  $A''$  components. Since our studies show very clear critical slowing down of the depolarized CP near  $T_4$ , it is very likely that instability of the  $A''$  mode triggers the transition at  $T_4$  and the symmetry decreases to  $C_1$ . If this is the case, the  $e_4$  spontaneous strain should appear below  $T_4$  and a clear anomaly in frequency shift of the TA mode corresponding to the  $c_{44}$  elastic constant should be observed. Clear acoustic anomaly for the  $c_{44}$  elastic constant is



also expected if the phase transition occurs from  $C_s$  into  $C_{2v}$  symmetry. Our results show that, indeed, a clear anomaly of the  $c_{44}$  is observed at  $T_4$ . Although the  $C_1$  symmetry is consistent with the dielectric studies and the present Brillouin studies, it is in contradiction with the established orthorhombic structure at room temperature.<sup>12</sup> On the other hand, the orthorhombic structure is consistent with the x-ray studies, but it is in contradiction with the dielectric studies and Brillouin selection rules (the TA modes are forbidden to be observed for the orthorhombic phase in back-scattering geometry). It is also worth noting that the phase transition at  $T_3$  has a first order character and it cannot be excluded that the point groups of the phases above and below  $T_3$  are not symmetry related. Therefore, the establishing of symmetries of the observed phases on the basis of the Brillouin studies is not conclusive and requires further investigations with other techniques.

Since the conductivity studies suggested that ionic conductivity is due to  $K^+$  ions, the x-ray structure determination showed that the main differences between the high- and low-temperature structures can be observed for the positions and thermal displacement factors of potassium and the present studies revealed that the CPs are correlated with strong increase in conductivity; it is plausible to assume that at higher temperatures the main contribution to the observed relaxation modes comes from motions of the potassium ions. However, at lower temperatures, both orderings in the potassium as well as niobium sublattice are responsible for polar ordering and the observed relaxation modes.

## V. CONCLUSIONS

Brillouin study revealed the presence of a number of weak acoustic anomalies associated with the ferroelectric phase transitions. Moreover, a very strong increase in damping and change in the slopes of the elastic constants as a function of temperature, resembling glass transition, have been observed near 690 K. These anomalies have been correlated with strong intensity increase in CPs, typical for superionic materials. These results give very strong arguments that the phase transition near  $T_3$  is associated with melting of the  $K^+$  sublattice and that KNBO exhibits superionic properties.

It has also been shown that the phase transitions at  $T_2$ ,  $T_3$ , and  $T_4$  are mainly of order-disorder type. The transition at  $T_2$  is connected with ordering of ions along the pseudohexagonal  $c$  axis and that at  $T_3$  is most likely induced by instability of the  $E''$ -symmetry mode. The phase transition at  $T_4$  is close to second order. It is induced by instability of the mode, which is also related to the  $E''$ -symmetry mode in the hexagonal phase and involves significant ionic motions normally to the  $c$  axis.

## ACKNOWLEDGMENTS

This work was done as a part of the Poland-Japan project. M. Maćzka acknowledges Tsukuba University for support of his stay in Japan and A. Hushur for help in the Brillouin measurements.

- 
- <sup>1</sup>A. A. Kaminskii, P. Becker, L. Bohaty, S. N. Bagaev, H. J. Eichler, K. Ueda, J. Hanuza, H. Rhee, H. Yoneda, K. Takaichi, I. Terashima, and M. Maczka, *Laser Phys.* **13**, 1385 (2003).
- <sup>2</sup>G. Aka, A. Kahn-Harari, F. Mougél, D. Vivien, F. Salin, P. Coquelain, P. Colin, D. Pelenc, and J. P. Damelet, *J. Opt. Soc. Am. B* **14**, 2238 (1997).
- <sup>3</sup>J. F. H. Nicholls, B. Henderson, and B. H. T. Chai, *Opt. Mater. (Amsterdam, Neth.)* **16**, 453 (2001).
- <sup>4</sup>X. B. Hu, J. Y. Wang, C. Q. Zhang, X. G. Xu, C. K. Loong, and M. Grimsditch, *Appl. Phys. Lett.* **85**, 2241 (2004).
- <sup>5</sup>A. A. Kaminskii, P. Becker, L. Bohaty, H. J. Eichler, A. N. Penin, K. Ueda, J. Hanuza, K. Takaichi, and H. Rhee, *Phys. Status Solidi A* **201**, 2154 (2004).
- <sup>6</sup>P. Becker, J. Schneider, and L. Bohaty, *Z. Kristallogr.* **S7**, 14 (1993).
- <sup>7</sup>P. Becker and L. Bohaty, *Z. Kristallogr.* **S9**, 28 (1995).
- <sup>8</sup>V. I. Voronkova, E. P. Kharitonova, V. K. Yanovskii, S. Yu. Stefanovich, A. V. Mosunov, and N. I. Sorokina, *Crystallogr. Rep.* **45**, 816 (2000).
- <sup>9</sup>E. P. Kharitonova, V. I. Voronkova, V. K. Yanovskii, and S. Yu. Stefanovich, *Neorg. Mater.* **38**, 978 (2002).
- <sup>10</sup>M. Maczka, D. Wlosewicz, P. E. Tomaszewski, and J. Hanuza, *Thermochim. Acta* **438**, 112 (2005).
- <sup>11</sup>J. Choisnet, D. Groult, and B. Raveau, *Acta Crystallogr., Sect. B: Struct. Crystallogr. Cryst. Chem.* **33**, 1841 (1977).
- <sup>12</sup>P. Becker, P. Held, and L. Bohaty, *Z. Kristallogr.* **211**, 449 (1996).
- <sup>13</sup>P. Becker, L. Bohaty, and J. Schneider, *Kristallografiya* **42**, 250 (1997).
- <sup>14</sup>B. A. Huberman and R. M. Martin, *Phys. Rev. B* **13**, 1498 (1976).
- <sup>15</sup>R. A. Field, D. A. Gallagher, and M. V. Klein, *Phys. Rev. B* **18**, 2995 (1978).
- <sup>16</sup>S. Furusawa, T. Suemoto, and M. Ishigame, *Phys. Rev. B* **38**, 12600 (1988).
- <sup>17</sup>S. Matsuo, H. Yugami, and M. Ishigame, *Phys. Rev. B* **48**, 15651 (1993).
- <sup>18</sup>S. Tsukada, Y. Ike, J. Kano, T. Sekiya, Y. Shimojo, R. Wang, and S. Kojima, *Appl. Phys. Lett.* **89**, 212903 (2006).
- <sup>19</sup>A. Hushur, H. Shigematsu, Y. Akishige, and S. Kojima, *Appl. Phys. Lett.* **86**, 112903 (2005).
- <sup>20</sup>F. M. Jiang and S. Kojima, *Appl. Phys. Lett.* **77**, 1271 (2000).
- <sup>21</sup>W. F. Oliver, C. A. Herbst, S. M. Lindsay, and G. H. Wolf, *Rev. Sci. Instrum.* **63**, 1884 (1992).
- <sup>22</sup>H. Z. Cummins and P. E. Schoen, in *Laser Handbook*, edited by F. T. Arecchi and E. O. Schultz-DuBois (North-Holland, Amsterdam, 1972).
- <sup>23</sup>R. Vacher and L. Boyer, *Phys. Rev. B* **6**, 639 (1972).
- <sup>24</sup>P. Kuzel, P. Moch, A. Gomez-Cuevas, and V. Dvorak, *Phys. Rev. B* **49**, 6553 (1994).
- <sup>25</sup>F. Furusawa, O. Chikagawa, S. Tange, T. Ishidate, H. Orihara, Y. Ishibashi, and K. Miwa, *J. Phys. Soc. Jpn.* **60**, 2693 (1991).

- <sup>26</sup>D. Eimerl, L. Davis, S. Velsko, E. K. Graham, and A. Zalkin, *J. Appl. Phys.* **62**, 1968 (1987).
- <sup>27</sup>A. G. Kalinichev, J. D. Bass, C. S. Zha, P. D. Han, and D. A. Payne, *J. Appl. Phys.* **74**, 6603 (1993).
- <sup>28</sup>H. Z. Cummins, in *Light Scattering Near Phase Transitions*, edited by H. Z. Cummins and A. P. Levanyuk (North-Holland, Amsterdam, 1983).
- <sup>29</sup>W. Schranz and D. Havlik, *Phys. Rev. Lett.* **73**, 2575 (1994).
- <sup>30</sup>A. Koreeda, T. Nagano, S. Ohno, and S. Saikan, *Phys. Rev. B* **73**, 024303 (2006).
- <sup>31</sup>T. Suemoto and M. Ishigame, *Phys. Rev. B* **32**, 4126 (1985).
- <sup>32</sup>K. B. Lyons and P. A. Fleury, *Phys. Rev. Lett.* **37**, 161 (1976).
- <sup>33</sup>M. Maczka, K. Hermanowicz, and J. Hanuza, *J. Phys.: Condens. Matter* **17**, 3355 (2005).
- <sup>34</sup>A. M. Pugachev, S. Kojima, and A. Hushur, *Phys. Status Solidi C* **11**, 3122 (2004).
- <sup>35</sup>M. Maczka, J. Hanuza, A. Majchrowski, and S. Kojima, *Appl. Phys. Lett.* **90**, 122903 (2007).
- <sup>36</sup>A. Nakajima, S. Shin, I. Kawaharada, and M. Ishigame, *Phys. Rev. B* **49**, 14949 (1994).
- <sup>37</sup>L. D. Landau and J. M. Khalatnikov, *Dokl. Akad. Nauk SSSR* **96**, 469 (1954).
- <sup>38</sup>M. E. Lines and A. M. Glass, *Principles and Application of Ferroelectrics and Related Materials* (Clarendon, Oxford, 1977), Chap. 8, p. 241.
- <sup>39</sup>M.-S. Zhang, T. Yagi, W. F. Oliver, and J. F. Scott, *Phys. Rev. B* **33**, 1381 (1986).
- <sup>40</sup>I. Tatsuzaki, M. Kasahara, M. Tokunaga, and H. Tanaka, *Ferroelectrics* **39**, 1049 (1981).
- <sup>41</sup>R. W. Gammon and H. Z. Cummins, *Phys. Rev. Lett.* **17**, 193 (1966).
- <sup>42</sup>R. L. Reese, I. J. Fritz, and H. Z. Cummins, *Phys. Rev. B* **7**, 4165 (1973).
- <sup>43</sup>M. Maczka, J. Hanuza, A. Majchrowski, and S. Kojima, *Phys. Rev. B* **75**, 214105 (2007).
- <sup>44</sup>H. Ledbetter, *Mater. Sci. Eng., A* **442**, 31 (2006).
- <sup>45</sup>L. Börjesson and L. M. Torell, *Phys. Rev. B* **36**, 4915 (1987).
- <sup>46</sup>A. I. Fedoseev, A. V. Svanidze, S. Kojima, and S. G. Lushnikov, *Mater. Sci. Eng., A* **442**, 224 (2006).